UMENTATION PAGE

Form Approved
OMB No. 0704-0188

2. REPORT DATE	3. REPORT TYPE AND DATES COVERED
1/July/93	Annual Technical 1/Jun/92-30/May/93

4. TITLE AND SUBTITLE

Surface Reactivity of Combustion Generated Soot Particles

5. FUNDING NUMBERS

PE - 61103D
PR - 3484
SA - S1
G - F49620-92-J-0314

6. AUTHOR(S)

Robert J. Santoro

7. PERFORMING ORGANIZATION NAME(S) AND ADDRESS(ES)

The Pennsylvania State University
240 Research Building East
University Park, PA 16802-2320

8. PERFORMING ORGANIZATION REPORT NUMBER

AFOSR-TR- 93 0601

9. SPONSORING/MONITORING AGENCY NAME(S) AND ADDRESS(ES)

AFOSR/NA
110 Duncan Avenue, Suite B115
Bolling AFB, DC 20332-0001

10. SPONSORING/MONITORING AGENCY REPORT NUMBER

11. SUPPLEMENTARY NOTES

12a. DISTRIBUTION/AVAILABILITY STATEMENT

Approved for public release; distribution is unlimited.

12b. DISTRIBUTION CODE

13. ABSTRACT *(Maximum 200 words)*

During the first year of this AASERT program, efforts have focused on the development of a sampling probe to extract soot particles from a laminar diffusion flame. Soot samples collected with this system are to be used to study the surface reactivity of the soot particles as a function of position in the flame. A suitable probe system has been developed and tested. Comparisons with laser-based measurements of percent conversion of fuel to soot show reasonable agreement. Additional studies have also been conducted to examine the applicability of laser-induced incandescence (LII) as a soot diagnostic. Results have demonstrated that the LII technique compares very well with previous measurements in a well-studied ethene/air laminar diffusion flame. Measurements of soot volume fraction, particle diameter and number density have been demonstrated.

14. SUBJECT TERMS

Soot particles, surface reactivity, gas turbines, diffusion flames, particle growth

15. NUMBER OF PAGES

38

16. PRICE CODE

17. SECURITY CLASSIFICATION OF REPORT	18. SECURITY CLASSIFICATION OF THIS PAGE	19. SECURITY CLASSIFICATION OF ABSTRACT	20. LIMITATION OF ABSTRACT
UNCLASSIFIED	UNCLASSIFIED	UNCLASSIFIED	UL

Annual Technical Report

on

Surface Reactivity of Combustion Generated Soot Particles

(AFOSR Grant F49620-92-J-0314)

Prepared by

Robert J. Santoro
Department of Mechanical Engineering
The Pennsylvania State University
University Park, PA 16802

Submitted to

Air Force Office of Scientific Research
Bolling Air Force Base
Washington, DC

July 1993

Table of Contents

Summary

During the first year of this AASERT program, efforts have focused on the development of a sampling probe to extract soot particles from a laminar diffusion flame. Soot samples collected with this system are to be used to study the surface reactivity of the soot particles as a function of position in the flame. A suitable probe system has been developed and tested. Comparisons with laser-based measurements of percent conversion of fuel to soot show reasonable agreement. Additional studies have also been conducted to examine the applicability of laser-induced incandescence (LII) as a soot diagnostic. Results have demonstrated that the LII technique compares very well with previous measurements in a well-studied ethene/air laminar diffusion flame. Measurements of soot volume fraction, particle diameter and number density have been demonstrated.

1.0 Introduction

Over the past decade, significant progress has been made in understanding the processes which control the formation, growth and burnout of soot particles in combustion systems. Because the presence of soot particles has significant effects on radiative transfer in gas turbine engines, combustor lifetime is seriously impacted by increases in soot formation as new engine technologies are developed. Consequently, AFOSR has had a continued effort in the study of soot particle formation aimed at understanding the fundamental processes which control its formation, growth and burnout. During the past five years, an extensive program to understand these processes in laminar diffusion flames has been ongoing in our laboratory at Penn State under AFOSR support. This program has emphasized in situ diagnostics to study the chemical and physical mechanisms important in the formation and oxidation processes associated with soot particles in combustion systems. These studies have led to one of the most extensive data bases available on the effects of fuel structure, species concentration, operating pressure, residence time and temperature on the processes which control soot formation. The present effort is complementing that program by adding a study aimed at investigating the surface reactivity of the soot particles as a function of these same parameters. An additional objective has emerged recently which deals with the development of a novel laser-based diagnostic technique for measuring soot particle size and concentration. This technique, which is based on laser heating effects to detect and characterize soot particles, will be described in this report as well.

The material which follows summarizes the progress made during the first year of this Augmentation Award for Science and Engineering Research Training.

2.0 Research Objectives

The soot formation process in combustion systems can be broadly described as: (1) a precursor chemistry stage in which the large chemical species which lead to the first particles are formed; (2) an inception stage in which a large number of small particles are formed; (3) a surface growth and coagulation stage in which most of the mass is added and particle size increases dramatically; and finally (4) an oxidation stage in which particle burnout can occur. In the present research effort, it is the second stage which is of particular interest.

Recent studies[1-4] of the surface growth process for soot particles have come to a series of differing conclusions. Although it is generally believed that acetylene (C_2H_2) is the predominant surface growth species in terms of mass addition, the specific mechanism responsible for the surface

reactions is not known. Conversely, there is some evidence to indicate that possibly large polynuclear aromatic hydrogen species (PAH) can also have a significant effect.[5] The current controversy centers on the role that the particle surface area has in the growth mechanism. Some experiments observe a direct dependence on particle surface area,[3] while others show little or no dependence.[4] Furthermore, in all combustion systems, as the soot particles age in the high temperature environment, they are observed to decrease in surface reactivity. Recent papers attempting to resolve this situation have focused on the concept of active sites[1,2] on the particle surface. It is then the number of these sites which controls the growth rate. As reactions occur at the active sites, they are removed and must be regenerated.[2] Thus, the lost of surface reactivity would be a result of a decrease in the regeneration mechanism. Some success has been achieved using this approach,[1,2] but there is no direct measurement support for the details of this mechanism.

Based on the above brief review of the current controversy regarding soot particle surface growth, the present study is aimed at directly measuring the variation in the particle surface reactivity in laminar diffusion flames. In this study, soot particles will be extracted from the flames and analyzed to determine the relative state of the particle surface properties. Conditions are carefully selected to correspond to previous well measured laminar diffusion flames studied in our laboratory. In fact, a series of ethylene flames which have been most extensively characterized[6] are being studied first. The initial measurements will emphasize soot mass yield, electron spin resonance (ESR) and total surface area (BET) as a function of axial position in the flame. The ESR measurements will yield information on the chemical radical activity of the soot particles[7] which we argue is related to the number of surface active sites. The BET surface area measurements will yield additional information on the manner in which the surface area available for reaction is changing. These measurements can be used to compare with optical light scattering measurements of this same quantity obtained for these flames in previous studies,[6] as well as for comparison with recent aggregate interpretations of that data.[8] Other surface sensitive measurements will be pursued as capabilities are identified.

3.0 Research Accomplishments

During the first year of the current AASERT program, efforts have been focused on the development of a suitable soot particle sampling technique. Additionally, recent efforts have considered the application of laser-induced incandescence for the determination of soot particle properties in the flames studied. Progress in both of these areas will be summarized below.

3.1 Sampling of Soot Particles in Laminar Diffusion Flames

A careful review of previous approaches for obtaining particle samples from reacting flows was undertaken initially. This review does not identify any previously proven techniques for accomplishing the objectives of the current studies which requires that samples in large quantities (0.1 gms) be potentially obtainable. However, previous work did provide some insights into appropriate approaches to be tried.

Three sampling approaches were identified for testing: (1) a dilution probe, (2) a honeycomb quenching system, and (3) a mixing quench system with subsequent soot collection. Only the dilution probe and mixing quench system have been examined to date.

The dilution probe is shown in Figure 1. This probe consists of two concentric brass tubes whose inner diameters were 9.6 mm (3/8") and 12.7 mm (1/2"), respectively. The inner tube was used to collect the soot particles, while the outer tube was employed to provide a flow of gaseous nitrogen to cool and dilute the soot particles sampled from the flame. The dilution with nitrogen is intended to quench any growth or oxidation reactions which could affect the soot particles following sampling. The nitrogen quench flow was introduced just after the probe inlet through four small holes drilled in the inner tube, as indicated in Figure 1. The entire length of the probe was approximately two feet.

The inner tube of the probe was connected to a filter holder which served as the trap to collect soot particles. Flow through the probe was induced by a vacuum pump. A critical orifice was placed between the soot particle trap and the vacuum pump which maintained the volumetric flow rate at approximately 10 L/min. A pressure gauge was placed between the soot trapped and the vacuum pump to monitor the pressure drop across the filter as soot particles were collected. The filters used in the experiments to date were Pallflex T60A20 Teflon-coated glass fiber filters.

Before discussing the results obtained using the dilution probe, it would be useful to describe the mixing quench system. Results obtained with this system affected the experiments undertaken using the dilution probe. The mixing quench system consists of a burner and soot sampling system, as shown in Figure 2. For the present study, a burner housing machined from 50.8 mm (2") diameter brass was used into which a quartz chimney was fitted of inner diameter 25.4 mm (1") which provided the outer air flow passage. It was convenient to use nominal 12.7 mm (1/2") brass tubing for the fuel tube. The length of the fuel tube was about 50 cm (~2') which ensured laminar flow at the outlet and also allowed variation of the flame position with respect to the tripper plate (see Fig. 2). The height of the fuel tube can be adjusted by loosening a compression fitting which is screwed into the base of the burner.

The air flow enters the base of the annular region, flows through a 2 cm layer of 3 mm diameter glass beads, and then through six layers of 70 gauges screen to provide laminar air flow. The inner glass tube (quartz) fits against the top of the screen located about 6 cm below the fuel tube. This quartz tube is sealed to the outer brass surface with teflon tape.

The outer glass tube, which serves as a concentric dilution tube, is sealed to the outer burner tube with an O-ring. The two dilution tubes were fitted with polished flanges to minimize leaks and to facilitate assembly. The purpose of the dilution tube is to provide uniform mixing of the smoke and gases and to cool or quench the smoke particulate prior to collection with minimal deposition on the walls. The dominant mechanism of smoke particulate deposition in this system is via thermophoresis, which is proportional to the temperature gradient near the wall. Cooling by rapid dilution by N_2 reduces the temperature gradient and, consequently, the particle deposition relative to cooling by only heat exchange with the walls of the tube.

The nominal N_2 flow rate is 590 cm^3/s (35.4 L/min), which dilutes the combustion product by a factor of 2 to a factor of 30 depending on the combustion air flow rate. The combustion products mix with the N_2 as they pass through a tripper plate. Visual observation of scattered light from a laser beam passing through the diluted combustion products indicated that for a 50.8 mm (2") diameter tube, a tripper plate with a 19.1 mm (3/4") orifice provided good mixing at a dilution flow rate of 590 cm^3/s (35.4 L/min).

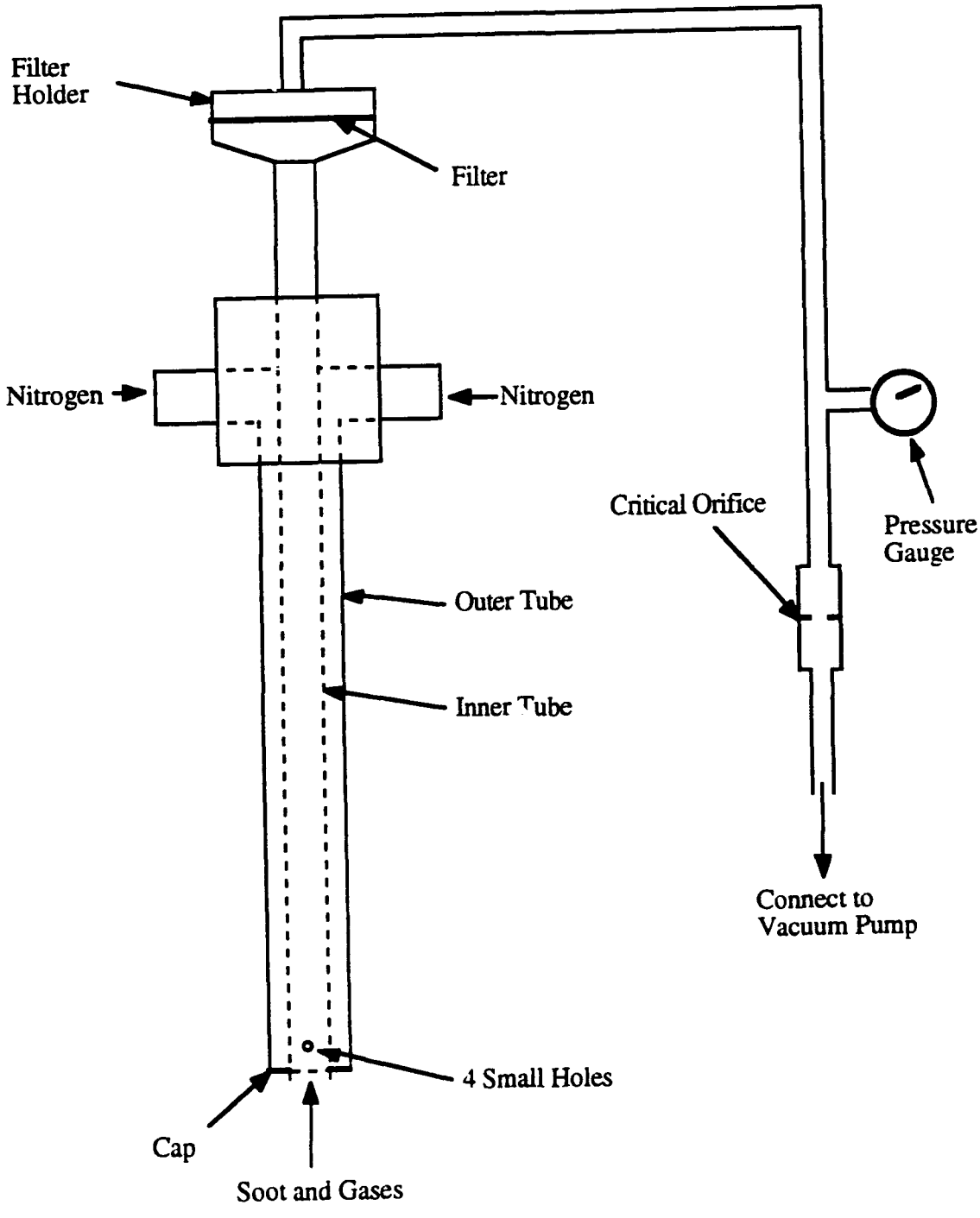

Figure 1. Diagram of the dilution probe and soot sampling assembly

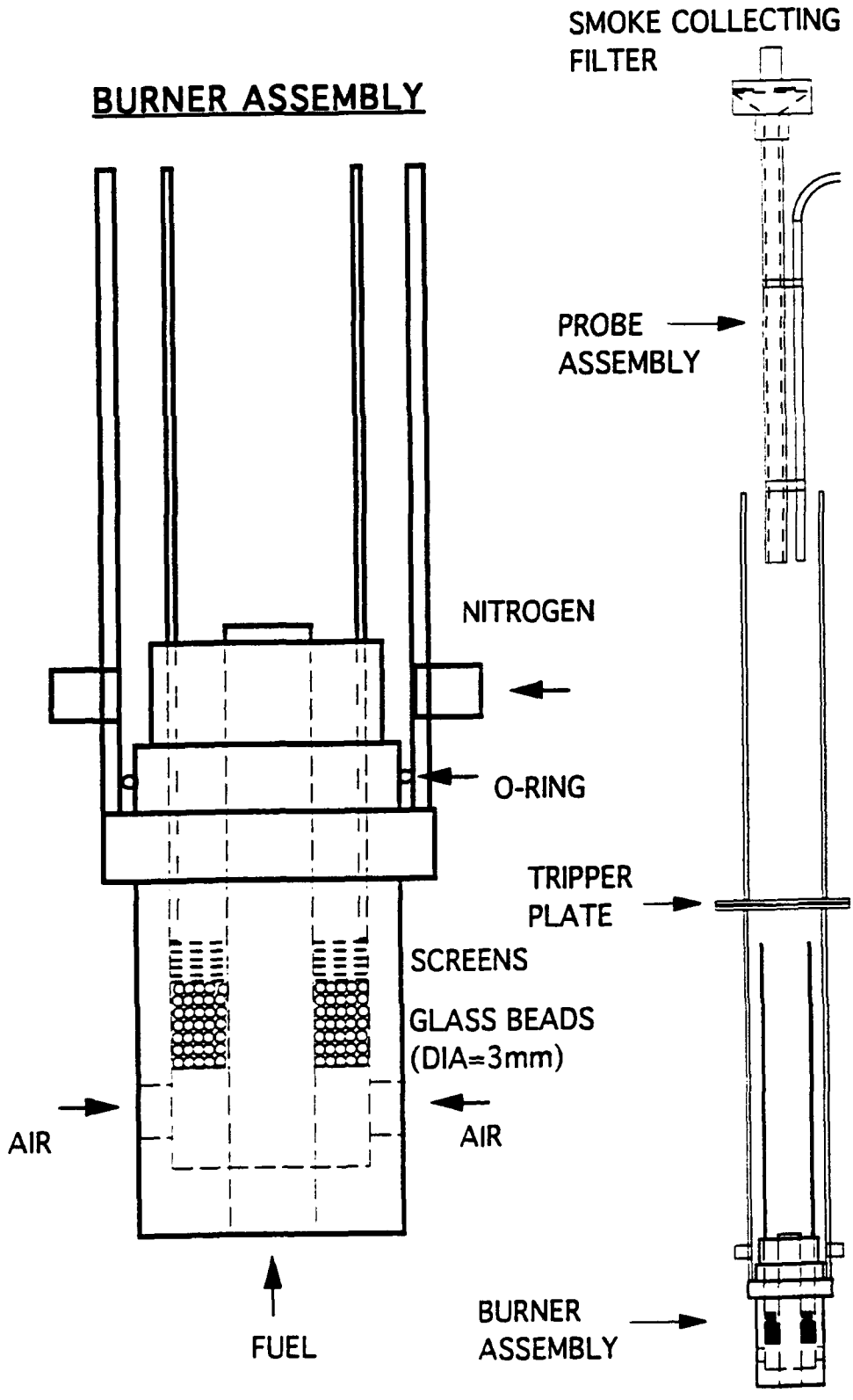

Figure 2. Diagram of the mixing quench burner and collection system

The concept behind the mixing quench system involved adjusting the fuel tube position such that the desired flame sampling location was located at the tripper plate position. The nitrogen introduced following the tripper plate would then quench the soot process and soot could then be collected downstream. Unfortunately, this approach gave poor results due to difficulties encountered in rapidly introducing the nitrogen quench gas without affecting the flame region below the tripper plate. However, in the course of studying this technique for collecting soot, it was observed that simply placing a wire mesh screen at the desired sampling point quenched the flame quite effectively. It was then decided to use this method with the existing burner and inner quartz tube to quench the soot and then sample the soot particles with the dilution probe. Thus, the new experimental apparatus consisted of the burner, an inner glass tube and an outer glass tube to support the screen (as shown in Fig. 3), followed by the dilution probe which was used to collect the soot particles.

The experimental procedure was to adjust the height of the burner fuel tube such that the desired sampling height in the flame corresponded to the location of the screen. A preweighed filter was then used to collect soot with the dilution probe located approximately 3 mm above the screen. The screen was slowly translated across the chimney to prevent soot clogging of the screen from affecting the flame. Soot was collected until the pressure drop across the filter was 20-25 inches of water. The time period over which the soot collection occurred was also determined. The mass of soot collected was then determined by weighting the filter.

With the mass of soot collected and the time period for the collection recorded, the mass flow rate of soot was calculated. Since the mass flow rate of the fuel is known, the % conversion of fuel to soot can be determined as:

$$\%\,\text{conversion} = \frac{\text{soot mass flow rate}}{\text{fuel mass flow rate}} * 100$$

Soot was collected as a function of height for an ethene/air diffusion flame with a fuel flow rate of 3.85 cm^3/s and an air flow rate of 233.3 cm^3/s. Several test runs were made with this system in which the nitrogen dilution was varied. The amount of nitrogen dilution flow was observed to have a 5-10% effect on the amount of soot collected when varied from a flow rate of zero to 100 cm^3/s. Although this effect is not large, it merits some further investigation.

Because of the observed effect of the nitrogen dilution flow, a profile of the soot field in the ethene/air diffusion flame was obtained for a zero dilution flow rate. Soot was collected at several heights in the flame and the percent conversion was calculated as described above. The results are given in Table 1 and are plotted in Figure 4 for the percentage conversion as a function of the non-dimensional height, η,

$$\eta = \frac{zD}{V} \ln(1 + 1/S)$$

where z is the height in the flame (cm), D is the diffusion coefficient for ethene (0.156 cm^2/s), V is the fuel flow rate (cm^3/s) and S is the air-to-fuel ratio for complete combustion (14.28 for ethene).

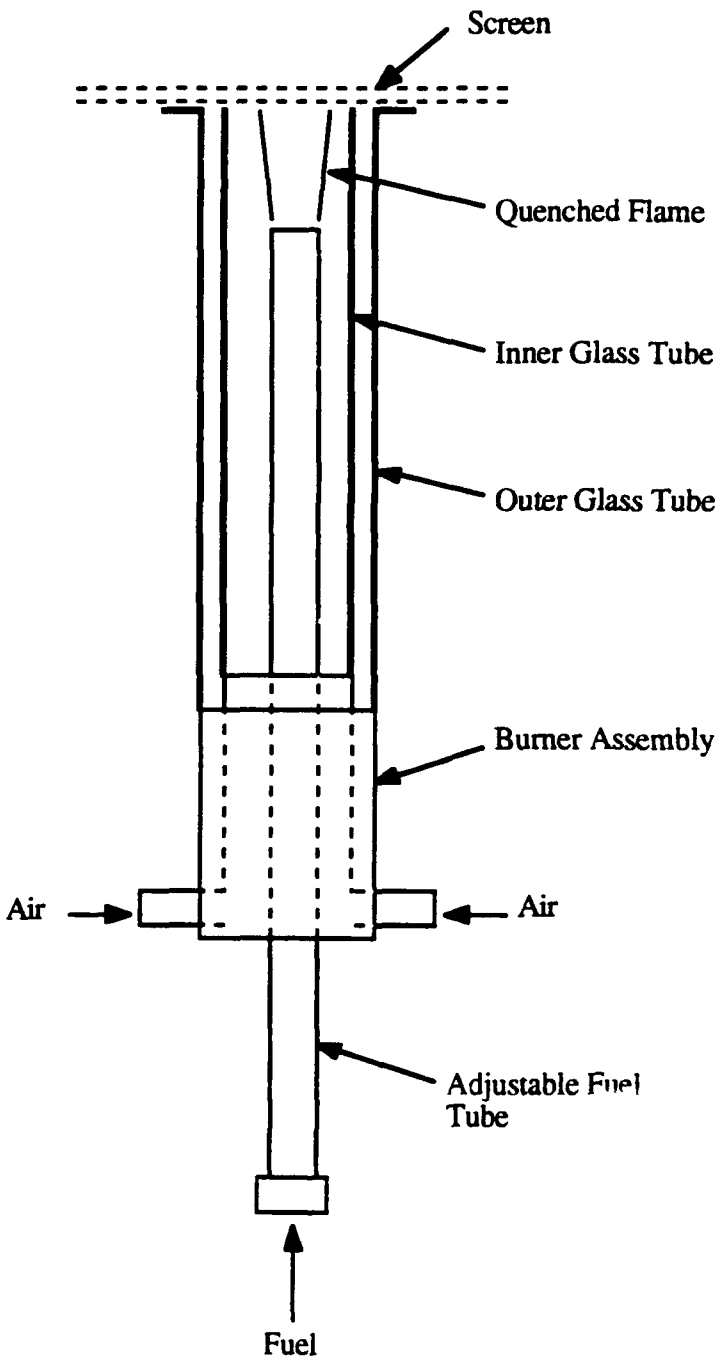

Figure 3. Modified soot burner and quench system

Table 1

Height mm	η	Soot Mass Flow $*10^{-4}$ (g/s)	% Conversion Fuel to Soot
2	0.0005	0.019	0.22
10	0.0027	0.413	4.71
18	0.0049	0.359	4.10
26	0.0071	1.32	15.06
34	0.0093	2.09	23.81
42	0.0115	2.09	23.81
50	0.0137	1.74	19.89
58	0.0159	1.32	15.09
66	0.0181	0.443	5.05
74	0.0203	0.104	1.18
82	0.0225	0.0	0.00

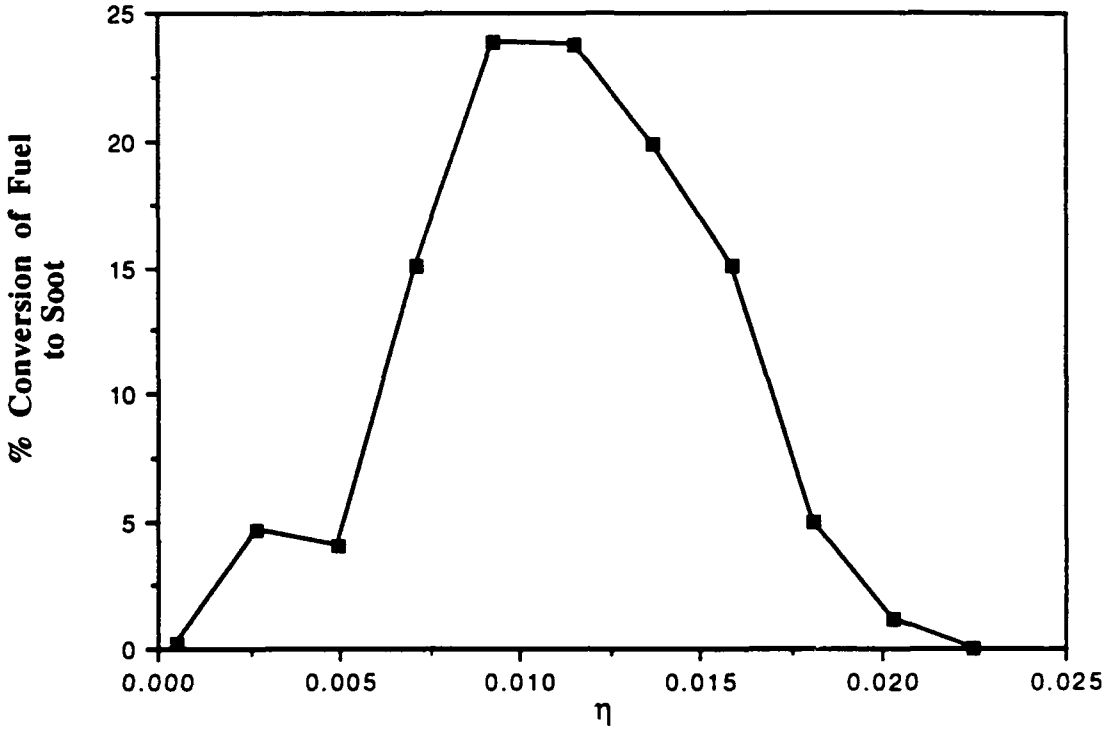

Figure 4. Percent conversion of fuel (ethene) to soot as a function of the non-dimensional height, η

The results shown in Figure 4 have the same trend as observed in the laser scattering measurements.[6] They show that soot is first formed low in the flame and then increases with increasing height reaching a maximum near $\eta = 0.01$. This location for the maximum % conversion of fuel to soot is in agreement with the previous studies of this flame.[6] The peak % conversions are higher in the present measurements than in the previous laser scattering/extinction studies (23.8% vs. 14%).[6] However, the soot sampling measurements reported here have not been subjected to heating prior to weighting to eliminate condensed water and organic species also trapped on the filter. Thus, the larger % conversions may result from this effect, which will be investigated in the future.

In summary, an attractive soot sampling approach has been developed which provides a means to collect soot formed in a diffusion flame as a function of axial location. Measurements show good qualitative agreement with previous measurements employing laser-based approaches. Future work will emphasize improving the quantitative capability of the technique.

3.2 Laser-Induced Incandescence

Laser-induced incandescence originates from the heating of soot particles to temperatures above the surrounding gas temperature due to the absorption of laser energy and subsequent blackbody radiation corresponding to the elevated soot particle temperature. The temperature of the soot particle is determined by the rate of laser energy absorption, conductive heat transfer to the surrounding gas, soot vaporization, and radiative heat loss through blackbody radiation.[9] For example, a Nd:YAG pulsed laser beam of ca. 8 ns duration used in the present laser-induced incandescence measurements represents an energy source in the energy balance equation, and the soot particle temperature rapidly rises during the duration of the laser pulse as the soot particles absorb the laser energy. The heat sink term in this phase is the conductive and radiative heat loss to the surrounding gas, which is much smaller than the laser energy absorption rate for laser fluence levels relevant to laser-induced incandescence. Near a soot particle temperature of ca. 4000 K, which is close to soot vaporization point, the temperature rise is severely curtailed by the energy expended in the vaporization of soot particles,[9] although soot surface temperature as high as 5000 K has been observed for sufficiently large laser fluence. Subsequent to the laser pulse, the temperature of the soot particles gradually decrease due to the conductive and radiative heat loss.

The intensity of the laser-induced incandescence, or the blackbody radiation due to laser heating, for a single soot particle has a dependence on the soot particle temperature, detection wavelength, and the laser fluence. The total incandescence emitted from the soot particle surface has a fourth-order dependence on the soot particle temperature, while the spectral shape of the incandescence is determined by the Planck's law with the maximum in blackbody radiation occurring at the wavelength inversely proportional to the soot particle temperature according to the Wien's displacement law. Thus, the temporal variation in the laser-induced incandescence signal at a given detection wavelength qualitatively follows the soot particle temperature in time, with the exact functional relationship being determined by the processes described above.

Computations of the laser-induced incandescence in response to an idealized laser pulse based on the blackbody radiation laws and the soot particle energy balance have been performed by Melton[9] and Tait and Greenhalgh.[10] In particular, in the limit of high laser power and maximum soot particle temperature near its vaporization point, Melton[9] has shown that the intensity of the laser-induced incandescence signal for a group of soot particles has a dependence on mean soot particle diameter raised to the power of $(3 + 0.15\lambda_{det}^{-1})$, where λ_{det} is the detection wavelength. For λ_{det} between 400 - 700 nm, for example, the laser-induced incandescence signal is proportional to the mean soot

diameter raised to the power of 3.22 to 3.38, or approximately to the soot volume fraction; and this forms the basis for the current approach of using laser-induced incandescence for pointwise measurement of soot volume fraction.

In spite of the potentially significant applications of LII in soot diagnostics, no experimental verification of the LII technique in determining local soot volume fraction has been reported to date. Thus, a study of the potential of this technique for quantitatively determining the soot volume fraction and particle diameter fields in an ethene/air laminar diffusion flame has been undertaken. The details of the findings of this study are contained in Attachment 1 which will be submitted to *Combustion and Flame* for publication.

A summary of the important conclusions of the study are given below:

1. Laser-induced incandescence has been used to obtain spatially-resolved measurements of soot volume fraction in laminar diffusion flames, in which comparisons with laser scattering/extinction data yield excellent agreement for both radial profiles and integrated volume fraction. Thus, laser-induced incandescence can be used as an instantaneous, spatially-resolved diagnostic of soot volume fraction without the need for the conventional line-of-sight laser extinction method.

2. The temporal characteristics of the laser-induced incandescence signal is observed to involve a rapid rise in intensity followed by a relatively long (ca. 600 ns) decay period subsequent to the laser pulse, while the effect of laser fluence is manifest in linear and saturated response of the laser-induced incandescence signal with the transition occurring at a laser fluence of approximately 3×10^7 W/cm^2 for laser pulse of ca. 8 ns in duration.

3. Spectral response of the laser-induced incandescence involves a continuous spectrum in the visible wavelength range due to the blackbody nature of the emission, where the spectral response for 300-450 nm wavelength range indicates a soot surface temperature of ca. 5000 K with the spectrum continuing at a nearly level intensity up to 750 nm wavelength due to the multiplicity of the soot particle size in the probe volume.

4. Simultaneous measurements of vertically-polarized light-scattering yield encouraging results concerning the mean soot particle diameter and number concentration; thus significant applications exist in two-dimensional imaging and simultaneous measurements of laser-induced incandescence and light-scattering to generate a complete soot property characterization.

4.0 Conclusions

An appropriate soot particle sampling technique has been developed for extracting soot particles from laminar diffusion flames. Comparisons with previously determined percent conversion of fuel to soot mass show good qualitative agreement. Improved quantitative agreement, as well as characterization of the soot particle surfaces in terms of surface area and reactivity, are goals for the next year of the program.

Laser-induced incandescence has been used to obtain spatially-resolved measurements of soot volume fraction in a laminar diffusion flame, in which comparisons with laser scattering/extinction data yield excellent agreement. In addition, the laser-induced incandescence signal is observed to involve a rapid rise in intensity followed by a relatively long (ca. 600 ns) decay period subsequent to

the laser pulse, while the effect of laser fluence is manifest in linear and saturated response of the laser-induced incandescence signal with the transition occurring at a laser fluence of approximately 3 x 10^7 W/cm^2. Spectral response of the laser-induced incandescence involves a continuous spectrum in the visible wavelength range due to the blackbody nature of the emission. Simultaneous measurements of laser-induced incandescence and light-scattering yield encouraging results concerning the mean soot particle diameter and number concentration. Thus, laser-induced incandescence can be used as an instantaneous, spatially-resolved diagnostic of soot volume fraction without the need for the conventional line-of-sight laser extinction method, while potential applications in two-dimensional imaging and simultaneous measurements of laser-induced incandescence and light-scattering to generate a complete soot property characterization are significant.

5.0 References

1. Woods, I. T. and Haynes, B. S., "Soot Surface Growth at Active Sites," *Combustion and Flame*, 85, pp. 523-525 (1991).

2. Frenklach, M. and Wang, H., "Detailed Modeling of Soot Particle Nucleation and Growth," *Twenty-Third Symposium (International) on Combustion*, The Combustion Institute, Pittsburgh, PA, pp. 575-582 (1990).

3. Harris, S. J. and Weiner, A. M., "Surface Growth of Soot Particles in Premixed Ethylene Air Flames," *Combustion Science and Technology*, 31, pp. 155-167 (1983).

4. Wieschnowsky, U., Bookhorn, H. and Fetting, F., "Some Observations Concerning the Mass Growth of Soot in Premixed Hydrocarbon-Oxygen Flames," *Twenty-Second Symposium (International) on Combustion*, The Combustion Institute, Pittsburgh, PA, pp. 343-352 (1988).

5. Howard, J. B., "Carbon Addition and Oxidation Reactions in Heterogeneous Combustion and Soot Formation," *Twenty-Third Symposium (International) on Combustion*, The Combustion Institute, Pittsburgh, PA, pp. 1107-1127 (1990).

6. Santoro, R. J., Yeh, T. T., Horvath, J. J. and Semerjian, H. G., "The Transport and Growth of Soot Particles in Laminar Diffusion Flames," *Combustion Science and Technology*, 53, p. 89 (1987).

7. Wagner, H. Gg., "Soot Formation in Combustion," *Seventeenth Symposium (International) on Combustion*, The Combustion Institute, Pittsburgh, PA, pp. 3-19 (1979).

8. Dobbins, R. A., Santoro, R. J. and Semerjian, H. G., "Analysis of Light Scattering From Soot Using Optical Cross Sections for Aggregates," *Twenty-Third Symposium (International) on Combustion*, The Combustion Institute, Pittsburgh, PA, pp. 267-275 (1988).

9. Melton, L. A., "Soot Diagnostics Based on Laser Heating," *Appl. Opt.*, 23, pp. 2201-2208 (1984).

10. Dasch, C. J., "Continuous-Wave Probe Laser Investigation of Laser Vaporization of Small Soot Particles in a Flame," *Appl. Opt.*, 23, pp. 2209-2215 (1984).

11. Tait, N. P. and Greenhalgh, D. A., "2D Soot Field Measurements by Laser Induced Incandescence," *Proceedings of the "Optical Methods and Data Processing In Heat Transfer and Fluid Flow" Conference*, London, April 1992.

6.0 Publications

Quay, B., Lee, T.-W. and Santoro, R. J., "Spatially-Resolved Measurements of Soot Volume Fraction Using Laser-Induced Incandescence," submitted to *Combustion and Flame*.

7.0 Meetings and Presentations

"Soot Formation Progress and Challenges," invited seminar, Allison Gas Turbines, February 11, 1993.

"Soot Formation Workshop," AFOSR Contractors' Meeting in Air Breathing Combustion, June 14, 1993.

8.0 Participating Personnel

Dr. Robert Santoro, Professor of Mechanical Engineering
Mr. Bryan Quay, Graduate Student, Department of Mechanical Engineering
(Ph.D. expected July, 1995)
Mr. Gregory Davis, Undergraduate Student, Department of Electrical Engineering
Ms. Vicki Jacobs, Undergraduate Student, Work Study, Lab Assistant
Mr. Matthew Schneider, Undergraduate Student, Undergraduate Summer Research Program in Mechanical Engineering

9.0 Interactions

Lubrizol, Wickeliffe, OH - Dr. Ralph Kornbrekke

Discussions with Dr. Kornbrekke have been pursuing the potential to undertake a collaborative research program to examine surface reactivity of soot particles which are formed under conditions of interest to Diesel engine combustion. The objective of this research would be to characterize the soot particle surfaces to allow development of appropriate additives which would suppress the deleterious effects of soot in engine lubrication.

10. Inventions

No inventions have resulted during the first year of this program.

Attachment 1

SPATIALLY-RESOLVED MEASUREMENTS OF SOOT VOLUME FRACTION USING LASER-INDUCED INCANDESCENCE

B. Quay, T.-W. Lee and R. J. Santoro
Department of Mechanical Engineering
The Pennsylvania State University
University Park, PA 16802

Abstract- Laser-induced incandescence is used to obtain spatially-resolved measurements of soot volume fraction in a laminar diffusion flame, in which comparisons with laser scattering/extinction data yield excellent agreement. In addition, the laser-induced incandescence signal is observed to involve a rapid rise in intensity followed by a relatively long (ca. 600 ns) decay period subsequent to the laser pulse, while the effect of laser fluence is manifest in linear and saturated response of the laser-induced incandescence signal with the transition occurring at a laser fluence of approximately 3×10^7 W/cm^2. Spectral response of the laser-induced incandescence involves a continuous spectrum in the visible wavelength range due to the blackbody nature of the emission. Simultaneous measurements of laser-induced incandescence and light-scattering yield encouraging results concerning the mean soot particle diameter and number concentration. Thus, laser-induced incandescence can be used as an instantaneous, spatially-resolved diagnostic of soot volume fraction without the need for the conventional line-of-sight laser extinction method, while potential applications in two-dimensional imaging and simultaneous measurements of laser-induced incandescence and light-scattering to generate a complete soot property characterization are significant.

INTRODUCTION

Formation, growth and oxidation of soot particles in diffusion flames involve a complex interaction between chemistry and fluid mechanics; and understanding of these chemical and physical processes is important not only from a fundamental scientific standpoint, but also due to applications in practical combustion devices. For example, soot emission from automotive and gas turbine engines constitutes one of the major pollutants that need to be minimized, while excessive soot formation and radiation in propulsion devices have adverse effects on combustor and flow components. In this regard, sooting characteristics of both turbulent and laminar flames have been investigated by numerous researchers, while in this laboratory attention has been focused on axisymmetric laminar diffusion flames. The soot property measurements made in this flame, thus far, involve the laser scattering/extinction method, which yields soot volume fraction, mean soot particle diameter, and number density after tomographic inversion of the laser extinction data due to the line-of-sight nature of these measurements.

However, recent studies of a process involving laser-induced incandescence (LII), in which the soot particles are heated up by the laser energy and emit blackbody radiation or incandescence at elevated temperatures, has shown that LII can be used as a non-intrusive spatially-resolved soot diagnostic [1-5]. In particular, it has been pointed out by Melton [1] that the LII signal is nearly proportional to the local soot volume fraction for sufficiently large laser fluence; thus, a pointwise measurement of soot volume fraction can be made without the need for the line-of-sight laser extinction and time-consuming tomographic inversion method. While other applications of LII in soot diagnostics, for measurements of soot particle size distribution for example, have been suggested [1], the most direct and significant application of LII may be in obtaining point measurements of soot volume fraction since the line-integral nature of laser extinction and subsequent tomographic inversion technique have deficiencies in some laminar flame and most turbulent flame configurations. For example, instantaneous measurements of local soot volume fraction can be made in turbulent diffusion

flames using LII without being limited to time-averaged data or axisymmetric burner geometry. Furthermore, applications of LII in investigations of soot properties include two-dimensional imaging of soot volume distributions and simultaneous LII and light-scattering measurements to construct a complete soot property characterization.

In spite of these potentially significant applications of LII in soot diagnostics, no experimental verification of the LII technique in determining the local soot volume fraction has been reported to date. The objective of this investigation, therefore, is to experimentally determine the applicability of the LII method in spatially-resolved measurements of soot volume fraction, to study the feasibility of making simultaneous LII and light-scattering measurements to obtain a complete soot property characterization, as well as to investigate the detailed characteristics of LII in laminar diffusion flames.

LASER-INDUCED INCANDESCENCE

Laser-induced incandescence originates from the heating of soot particles to temperatures above the surrounding gas temperature due to the absorption of laser energy and subsequent blackbody radiation corresponding to the elevated soot particle temperature. The temperature of the soot particle is determined by the rate of laser energy absorption, conductive heat transfer to the surrounding gas, soot vaporization, and radiative heat loss through blackbody radiation [1,2]. For example, a Nd:YAG pulsed laser beam of ca. 8 ns duration used in the present laser-induced incandescence measurements represents an energy source in the energy balance equation, and the soot particle temperature rapidly rises during the duration of the laser pulse as the soot particles absorb the laser energy. The heat sink term in this phase is the conductive and radiative heat loss to the surrounding gas, which is much smaller than the laser energy absorption rate for laser fluence levels relevant to laser-induced incandescence. Near a soot particle temperature of ca. 4000 K, which is close to soot vaporization point, the temperature rise is severely curtailed by the energy expended in the vaporization of soot particles [1], although soot surface temperature as high as 5000 K has been

observed for sufficiently large laser fluence [6]. Subsequent to the laser pulse, the temperature of the soot particles gradually decrease due to the conductive and radiative heat loss.

The intensity of the laser-induced incandescence, or the blackbody radiation due to laser heating, for a single soot particle has a dependence on the soot particle temperature, detection wavelength, and the laser fluence. The total incandescence emitted from the soot particle surface has a fourth-order dependence on the soot particle temperature, while the spectral shape of the incandescence is determined by the Planck's law with the maximum in blackbody radiation occurring at the wavelength inversely proportional to the soot particle temperature according to the Wien's displacement law. Thus, the temporal variation in the laser-induced incandescence signal at a given detection wavelength qualitatively follows the soot particle temperature in time, with the exact functional relationship being determined by the processes described above.

Computations of the laser-induced incandescence in response to an idealized laser pulse based on the above blackbody radiation laws and the soot particle energy balance have been performed by Melton [1] and Tait and Greenhalgh [4]. In particular, in the limit of high laser power and maximum soot particle temperature near its vaporization point, Melton [1] has shown that the intensity of the laser-induced incandescence signal for a group of soot particles has a dependence on mean soot particle diameter raised to the power of $(3 + 0.15\lambda_{det}^{-1})$, where λ_{det} is the detection wavelength. For λ_{det} between 400 - 700 nm, for example, the laser-induced incandescence signal is proportional to the mean soot diameter raised to the power of 3.22 to 3.38, or approximately to the soot volume fraction; and this forms the basis for the current approach of using laser-induced incandescence for pointwise measurement of soot volume fraction.

EXPERIMENTAL METHODS

The experimental apparatus involved a coannular laminar diffusion flame burner which was identical to the burner employed in this laboratory in previous studies of soot properties [7-9]; thus, only a brief description will be given here. The overventilated laminar flame burner consisted of two

concentric brass tubes with fuel and air flowing through the inner (11.1 mm ID) and outer (101.6 mm ID) tubes, respectively, where the fuel tube extended 4 mm beyond the exit plane of the air tube. Flow conditioning for the air was achieved via a layer of 3.0 mm glass beads, a series of wire screens and a ceramic honeycomb section, while the fuel passage contained a layer of 3.0 mm glass beads and a single wire screen. A 405 mm long brass cylinder that fit onto the outer tube was used as a chimney to shield the flame from laboratory air disturbances; and optical access was obtained through machined slots on the brass cylinder which traversed with the burner assembly. In addition, screens and a flow restrictor were placed at the chimney exit to achieve a highly stable flame similar to previous studies [7-9]. The traverse system involved a stepper motor and controller (Daedal PC-410-288) which provided positioning capability with a resolution of 0.25 mm.

The optical setup for the laser-induced incandescence included an Nd:YAG laser (Continuum Model NY61-10), the output beam of which was focused to a probe volume of approximately 0.5 mm in diameter using a bi-convex lens of 400 mm focal length. A schematic of the optical arrangement is shown in Fig. 1. Both the 1064 nm and frequency-doubled 532 nm beams from the Nd:YAG laser were used, the diameter of which prior to the focusing lens was approximately 9 mm with a nearly Gaussian profile. In order to observe the effect of variation of the laser fluence, a number of different combinations of neutral density filters were used to attenuate the laser energy by a varying amount. For example, by using combinations of neutral density filters with transmittances of 0.015, 0.2, 0.5 and 1.0 percent, laser energy ranging from 0.02 to 1.5 mJ were obtained corresponding to laser fluence between 9.3×10^5 and 8.8×10^7 W/cm^2. The laser energy was monitored during the experiment using a pyrometer (Molectron J1000), and was maintained during the actual measurements of the soot volume fraction at 1.5 mJ for a laser fluence of 8.8×10^7 W/cm^2 in order to minimize the effect of laser beam attenuation across the flame (see Fig. 5). The laser-induced incandescence signal was collected at a 90° angle using a focusing lens with f-number of 3 at unit magnification. A polarization filter was placed in front of the collection lens in order to minimize the interference from

light-scattering by passing only the signal with polarization perpendicular to that of the incident laser beam. Since the LII signal had a continuous spectrum in the visible wavelength range while interference from light-scattering and PAH fluorescence was expected near 532 nm and above [9,10], the detection of LII signal was made at 400 nm for both 532 nm and 1064 nm wavelength probe laser beams. Measurements made at 500 and 700 nm detection wavelengths for the 1064 nm wavelength probe laser yielded identical results due to the continuous nature of the LII spectrum in the visible wavelength range. The detection wavelength was set by using a 0.25m-monochromator (Instruments SA H20) with a grating blazed at 330 nm with 1 mm slits. The bandpass of the monochromator was estimated to be 4 nm FWHM, while the spectral response of the monochromator was calibrated using an incandescent lamp (Epley T24). A photomultiplier tube (Hammamatsu R928) was connected to the exit slit of the monochromator, the signal from which was conditioned using a boxcar integrator with a gate width of 5 ns and sample averaging of 30 laser shots.

Temporal variations of the LII signal were observable by moving the boxcar gate in 2-10 ns increments. LII profiles across the flame and spectral characteristics of the LII signal were observed by using the burner traverse system described above and by the scanning of the detection wavelength via the monochromator, respectively. The measurements were made in non-smoking ethylene/air diffusion flames where the ethylene and air flow rates were 3.85 cm^3 and 1060 cm^3/s, respectively.

RESULTS AND DISCUSSION

Figure 2 shows a typical temporal variation of the LII and vertically-polarized light-scattering signals taken at a height of 40 mm above the fuel tube exit for an ethylene laminar diffusion flame at the radial location where the peak soot volume fraction is observed (r=2.5 mm). The variation of the LII signal in time has been obtained by increasing the boxcar gate delay in 2-10 ns increments with respect to the laser pulse while averaging over 30 laser shots, as described above. It can be observed in Fig. 2 that the initial phase of the signal involves a rapid rise in the LII signal intensity due to the increase in soot temperature during the laser pulse of ca. 8 ns in duration. Subsequent to the peak in

LII signal, the soot particles undergo a conductive and radiative heat loss to the ambient gas and the LII signal gradually decreases, although a sensible LII signal is still observed at approximately 600 ns after the laser pulse. The temporal variation of the LII signal shown in Fig. 2 is qualitatively very similar to the LII response function for an idealized laser pulse computed by Melton [1]. A characteristic time constant for the LII process for soot particles has been shown to be linearly proportional to the soot particle diameter [3], and is estimated to be approximately 700 ns for a diameter of 100 nm. The decay time observed in Fig. 2 is approximately 600 ns for the signal to decrease to 10% of the peak value, while the mean soot particle diameter (D_{63}) at this location is approximately 135 nm (see Fig. 7(b)). Thus, in contrast to light-scattering signals, for example, which is observable only during the duration of the laser pulse due to its elastic scattering nature, the LII signal exhibits a much longer temporal characteristic as shown in Fig. 2. Melton [1] has discussed the potential for obtaining particle size distribution from the temporal behavior of the LII signal. Such information is better obtained using a shorter probe laser wavelength than that used in the present study and may also suffer from interference from laser-induced fluorescence from PAH species [1]. For the probe laser wavelength used in this study, the temporal response of the LII signal does not depend on the particle size [1].

A comparison between the soot volume fraction measured by LII and laser scattering/extinction technique is shown in Figs. 3 (a)-(c), where the soot volume fraction is plotted as a function of radial location at selected heights ranging from 10 to 70 mm above the fuel tube exit. The open and dark symbols represent laser scattering/extinction and LII data, respectively. The laser scattering/extinction data for soot volume fraction in this flame has been taken from Santoro et al. [7,8], and involves the well-known method of measuring the line-of-sight extinction of the laser beam followed by a tomographic inversion in order to reconstruct the local soot volume fraction. Further details of this technique and the data can be found in Santoro et al. [7,8]. In order to calibrate the observed LII signal, the LII signal at a single spatial point corresponding to the radial location where

the peak soot volume fraction occurs (r=2.5 mm) at the 40 mm height has been equated with the known value of soot volume fraction at this location from the laser scattering/extinction measurements. All other LII data can then be converted to absolute soot volume fraction based on this single-point calibration procedure.

The radial profiles of soot volume fraction obtained in this manner as shown in Figs. 3(a)-(c) exhibit the familiar physics of soot growth and oxidation in this flame. At low heights, soot particles are observed in the annular region on the fuel-rich side of the flame. Soot formed in this region undergoes net growth with increasing height up to H = 40 mm where the peak soot volume fraction is observed at radial location of 2.5 mm from the centerline, while soot is observable at the centerline at height of 30 mm in Fig. 3 (a). Subsequent development involves a net destruction of soot particles through soot oxidation with soot volume fraction at the annular region diminishing more rapidly than in the central region.

Figures 3 (a)-(c) show an excellent agreement between the LII and laser extinction/scattering data for the soot volume fraction with data being within 5-10% of one another at most of the heights where measurements have been obtained. However, there is a tendency for the LII data to underestimate the soot volume fraction on one side of soot peaks resulting in slightly asymmetric soot volume fraction profiles in Fig. 3 (b). This effect is more pronounced at the height of 40 mm than elsewhere, and is attributable to the fact that the LII signal from the far soot peak traverses the flame in order to arrive at the signal detection site and thus is subject to increased path length and correspondingly increased absorption of the signal by the soot and PAH species in the flame. This effect may be correctable by estimating and integrating the local extinction of the signal across the flame. Figure 4 similarly shows the integrated soot volume fraction as a function of height.[8] The LII data is again compared with laser extinction/scattering data, which yields reasonably good agreement. Due to the absorption of the LII signal from the far soot peak which leads to a slight asymmetry in the radial profiles and underestimation of the soot volume fraction on one side of the

soot peaks as noted above, the integrated soot volume fraction from LII measurements are slightly less than the laser extinction/scattering data in Fig. 4 with the maximum discrepancy being approximately 10% at a height of 30 mm.

The effect of laser fluence on the LII signal is shown in Fig. 5. The laser fluence has been varied from 9.3×10^5 to 8.8×10^7 W/cm^2 by using various combinations of neutral density filters, as described earlier. For laser fluence from 9.3×10^5 to 2×10^7 W/cm^2, it can be seen in Fig. 5 that the LII signal is nearly linear with respect to the variation in laser fluence. This is due to the fact that the soot particle temperature increases as a function of the laser fluence which causes a corresponding increase in LII. In contrast, the LII signal for laser fluence beyond ca. 3.0×10^7 W/cm^2 exhibits a very small increase with respect to an increase in laser fluence. The influx of laser energy on the soot particles can cause vaporization of small carbon fragments such as C_2 and C_3 from the soot particle surface, and for sufficiently large laser fluence this vaporization mechanism and corresponding mass loss can become the dominant effect which limits the increase in soot particle temperature and thus causes a leveling of the LII signal as shown in Fig. 5. However, the LII signal intensity in this "saturation" regime increases as a very weak function of the laser fluence in Fig. 5 similar to the results of Eckbreth [6] in which soot surface temperature as high as 5000 K is observed with increasing laser fluence. From extrapolation of data points in Fig. 5, it is estimated that the linear response of the LII with respect to laser fluence variations is limited to below 3×10^7 W/cm^2. During the actual measurements of soot volume fraction, large laser fluence levels in the saturation regime have the advantage of being least affected by the effects of the laser beam attenuation across the flame since the LII signal is a very weak function of the laser fluence in this regime.

The spectral response of the LII is shown in Fig. 6, where the LII signal is plotted as a function of the detection wavelength. The spectral scan of the LII signal has been obtained by rotating the grating in the monochromator so that the detection wavelength is varied in 10 nm increments. Measurements have been taken at the radial locations where the peak soot volume

fraction occurs at 40 mm height for a probe laser beam at 1064 nm wavelength with an energy of 1.5 mJ/pulse or laser fluence of 8.8×10^7 W/cm^2. For 1064 nm laser beam, interference from light-scattering and PAH fluorescence is minimal in the visible wavelength range, although a fortuitous peak at 532 nm is seen due to the leakage of 532 nm beam from the laser and corresponding light-scattering at this wavelength. It can be observed that as expected the LII signal exhibits continuous spectra in the visible wavelength range with the signals decreasing to small levels below 300 nm. The LII spectrum also shows no distinct peaks and continue up to 750 nm at a nearly constant level. Comparison with computed blackbody radiation curves, as shown in Fig. 6, indicates that the LII spectrum in the 300-450 nm range corresponds to soot temperature between 5000 and 6000 K, which is higher than the estimated soot vaporization temperature of ca. 4000 K. That the LII spectrum continues at a nearly constant level up to 750 nm and beyond, while the computed radiation curves begin to decline, is attributed to the fact that large soot number density and corresponding multiplicity of soot particle size is present in the probe volume with different soot surface temperatures induced by the laser fluence. Hence, a more continuous and level spectral response is expected as shown in Fig. 6 for a group of soot particles in comparison to a radiation curve computed for a single soot particle surface temperature. From Fig. 6, it can also be observed that using 1064 nm wavelength probe laser, LII measurements can be taken at nearly any wavelength in the visible range, except near 532 nm, due to the absence of interference from PAH fluorescence and light-scattering as noted above, and measurements taken at detection wavelengths of 400 and 700 nm have yielded identical soot volume fraction results.

Figure 7(a) shows the soot volume fraction measured by LII and the vertically-polarized component of the light-scattering signal (Q_{vv}), while Fig. 7 (b) contains the data for the mean soot particle diameter and the soot number density obtained from these measurements. The vertically-polarized light-scattering signal has been obtained for the 532 nm wavelength probe laser beam, and the calibration for the absolute value of Q_{vv} has been obtained by matching with the known value of

this signal at a single radial position using measurements by Santoro et al. [6] similar to the calibration procedure for the soot volume fraction. From the soot volume fraction and light-scattering data which is proportional to the 6th moment of the soot particle diameter distribution, the mean soot particle diameter (D_{63}) and the soot number density (N) can be obtained as follows [7]:

$$D_{63} = \lambda^{4/3} \left(\frac{2Q_{vv}}{3\pi^3 F(\tilde{m}) f_v} \right)^{1/3}, \text{ where} \tag{1}$$

$$F(\tilde{m}) = \left| \frac{\tilde{m}^2 - 1}{\tilde{m}^2 + 2} \right|^2. \tag{2}$$

$$N = \frac{12 f_v}{\pi D_{63}^3} \tag{3}$$

Here, f_v denotes the soot volume fraction while the complex index of refraction, $\tilde{m}$, is taken as (1.57 - 0.56 i) following Dalzell and Sarofirm [11]. The resultant mean soot particle diameter and the soot number density are again compared with the previous data obtained for this flame using the laser scattering/extinction method [7]. Figure 7 shows that the mean soot particle diameters are in very good agreement with the discrepancy being mostly limited to the central region where due to the relatively low signal levels there is the largest uncertainty in both the LII and light-scattering data. The mean soot particle diameter from LII data in the present study ranges from 75-130 nm, while diameters of 60 to 135 nm have been observed by Santoro et al. [7]. The soot number density profiles are similarly in reasonably good agreement with the discrepancy again occurring near the centerline. Since the number density is inversely proportional to the cube of the mean soot particle diameter, the factor of two difference in the soot number density near the centerline is caused by the corresponding difference in the mean soot particle diameter shown in Fig. 7(b). Thus, with a single-

point or two-dimensional measurements of LII and light-scattering which can be set up simultaneously with relative ease, a complete characterization of soot particle properties may be directly obtained.

CONCLUSIONS

From the discussion above, following conclusions concerning the laser-induced incandescence diagnostic of soot volume fraction are made:

(1) Laser-induced incandescence has been used to obtain spatially-resolved measurements of soot volume fraction in laminar diffusion flames, in which comparisons with laser scattering/extinction data yield excellent agreement for both radial profiles and integrated volume fraction. Thus, laser-induced incandescence can be used as an instantaneous, spatially-resolved diagnostic of soot volume fraction without the need for the conventional line-of-sight laser extinction method.

(2) The temporal characteristics of the laser-induced incandescence signal is observed to involve a rapid rise in intensity followed by a relatively long (ca. 600 ns) decay period subsequent to the laser pulse, while the effect of laser fluence is manifest in linear and saturated response of the laser-induced incandescence signal with the transition occurring at a laser fluence of approximately 3×10^7 W/cm^2 for laser pulse of ca. 8 ns in duration.

(3) Spectral response of the laser-induced incandescence involves a continuous spectrum in the visible wavelength range due to the blackbody nature of the emission, where the spectral response for 300-450 nm wavelength range indicates a soot surface temperature of ca. 5000 K with the spectrum continuing at a nearly level intensity up to 750 nm wavelength due to the multiplicity of the soot particle sizes in the probe volume.

(4) Simultaneous measurements of LII and the vertically-polarized light-scattering yield encouraging results concerning the mean soot particle diameter and number concentration; thus significant applications exist in two-dimensional imaging and simultaneous measurements of laser-induced incandescence and light-scattering to generate a complete soot property characterization.

ACKNOWLEDGEMENTS

This material is based upon work supported by the Air Force Office of Scientific Research under Award No. F49620-92-J-0314 with Dr. Julian Tishkoff as contract manager. The support of the Air Force Office of Scientific Research is gratefully acknowledged.

REFERENCES

1. Melton, L. A. *Appl. Opt.* 23:2201-2208 (1984).

2. Dasch, C. J. *Appl. Opt.* 23:2209-2215 (1984).

3. Eckbreth, A. C., Bonczyk, P. A. and Verdieck, J. F. *Prog. Energy Combust. Sci.* 5:253-322 (1979).

4. Tait, N. P. and Greenhalgh, D. A. *Proceedings of the "Optical Methods and Data Processing In Heat Transfer and Fluid Flow" Conference.* London, April 1992.

5. Dec, J. E., zur Loye, A. O. and Siebers, S. L. *SAE Technical Papers Series* SAE-910224. Society of Automotive Engineers, PA 1991.

6. Eckbreth, A. C. *J. Appl. Physics* 48:4473-4479 (1977).

7. Santoro, R. J., Semerjian, H. G. and Dobbins, R. A. *Combust. Flame* 51:203-218 (1983).

8. Santoro, R. J., Yeh, T. T., Horvath, J. J., and Semerjian, H. G. *Combust. Sci. and Tech.* 53:89-115 (1987).

9. Puri, R., Moser, M., Santoro, R. J. and Smyth, K. C. *Twenty-Fourth Symposium (International) on Combustion.* The Combustion Institute, Pittsburgh, 1992, pp. 1015-1022.

10. Miller, H. J., Mallard, G. W. and Smyth, K. C. *Combust. Flame* 47:205-214 (1982).

11. Dalzell, W. H. and Sarofim, A. F. *Trans. ASME J. Heat Transfer* 91:100-104 (1969).

Figure Captions

Fig. 1 Optical arrangement for laser-induced incandescence measurements.

Fig. 2 Temporal response of the laser-induced incandescence.

Fig. 3 Radial profiles of soot volume fraction obtained via laser-induced incandescence and laser scattering/extinction at (a) H = 10, 20, and 30 mm; (b) 40 and 50 mm; and (c) 60 and 70 mm.

Fig. 4 Integrated soot volume fraction plotted as a function of height.

Fig. 5 Effect of laser fluence on laser-induced incandescence signal.

Fig. 6 Spectral response of the laser-induced incandescence.

Fig. 7(a) Soot volume fraction and vertically-polarized light-scattering signals at H = 40 mm.

Fig. 7(b) Mean soot particle diameter and soot number concentration at H = 40 mm.

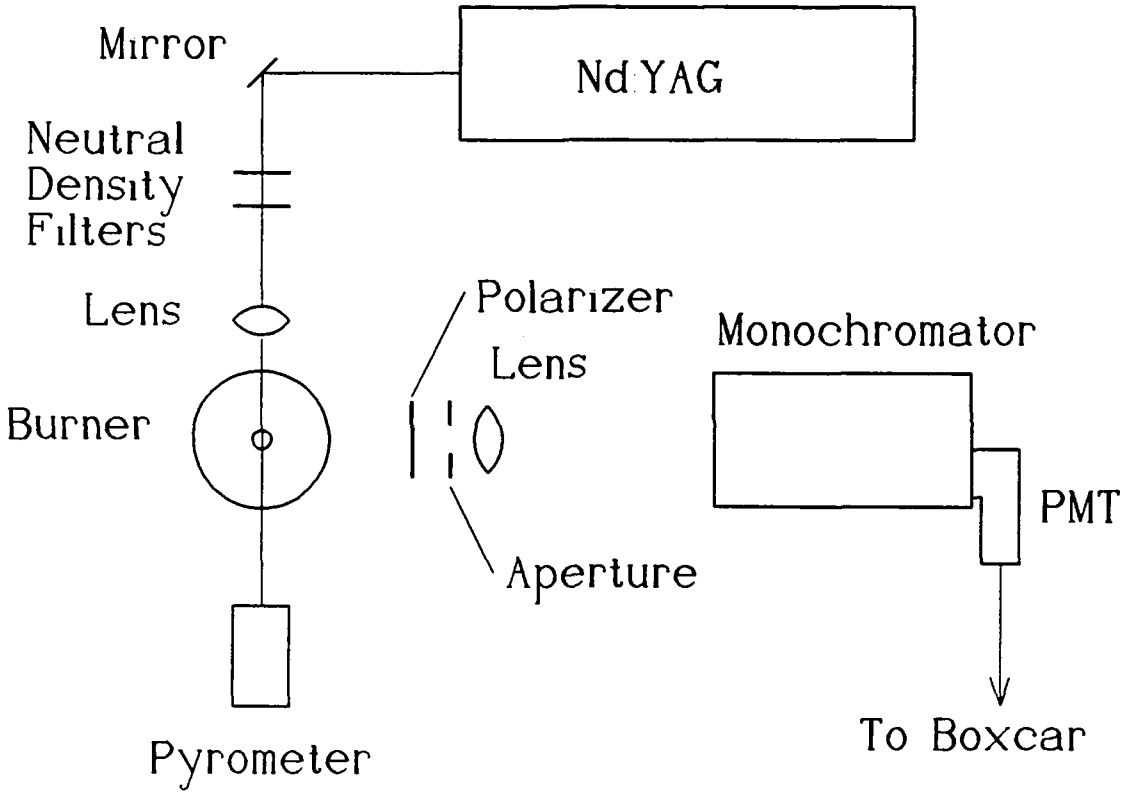
Mirror
Nd:YAG
Neutral
Density
Filters
Lens
Polarizer
Lens
Monochromator
Burner
PMT
Aperture
To Boxcar
Pyrometer

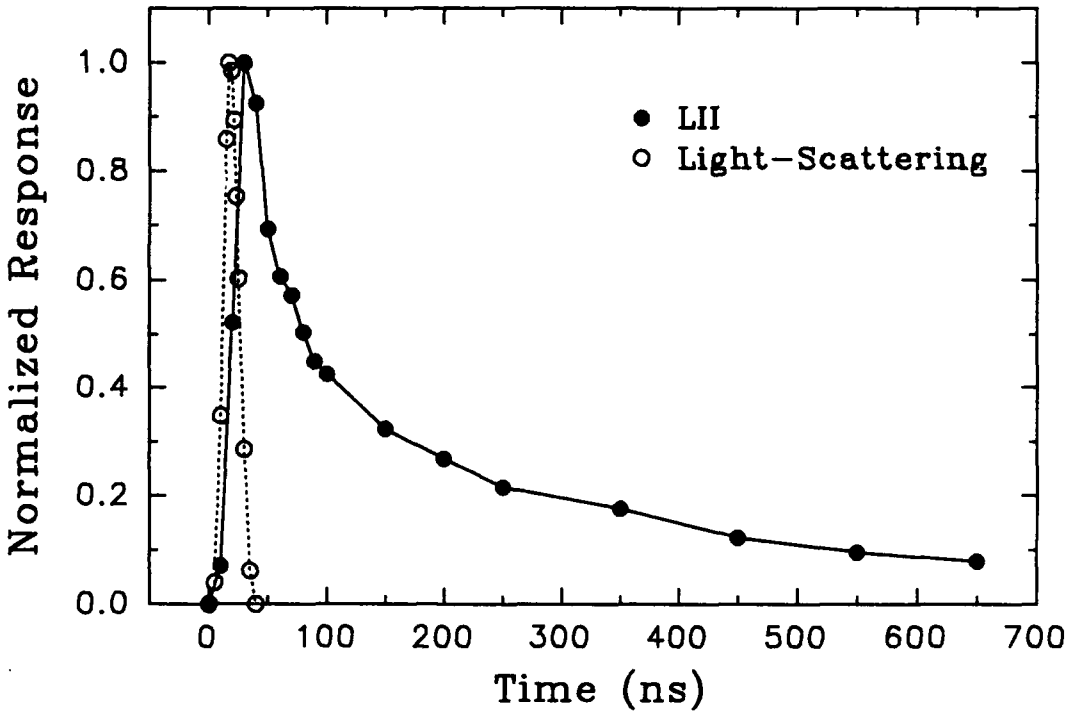
Normalized Response
1.0
0.8
0.6
0.4
0.2
0.0
0
100
200
300
400
500
600
700
Time (ns)
LII
Light–Scattering

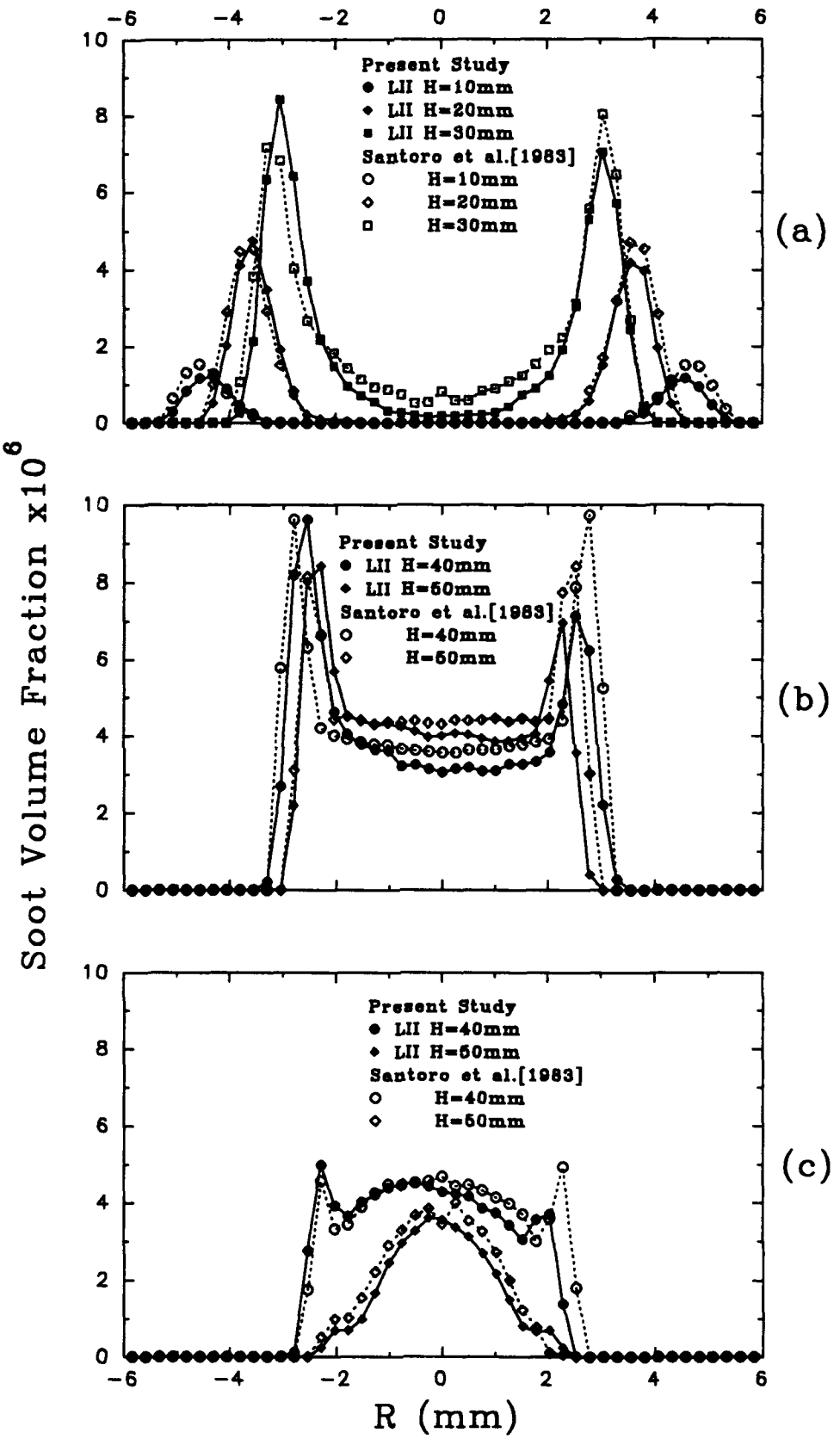
Present Study
LII H=10mm
LII H=20mm
LII H=30mm
Santoro et al.[1983]
H=10mm
H=20mm
H=30mm
(a)
Present Study
LII H=40mm
LII H=50mm
Santoro et al.[1983]
H=40mm
H=50mm
(b)
Present Study
LII H=40mm
LII H=50mm
Santoro et al.[1983]
H=40mm
H=50mm
(c)
Soot Volume Fraction x10^6
R (mm)

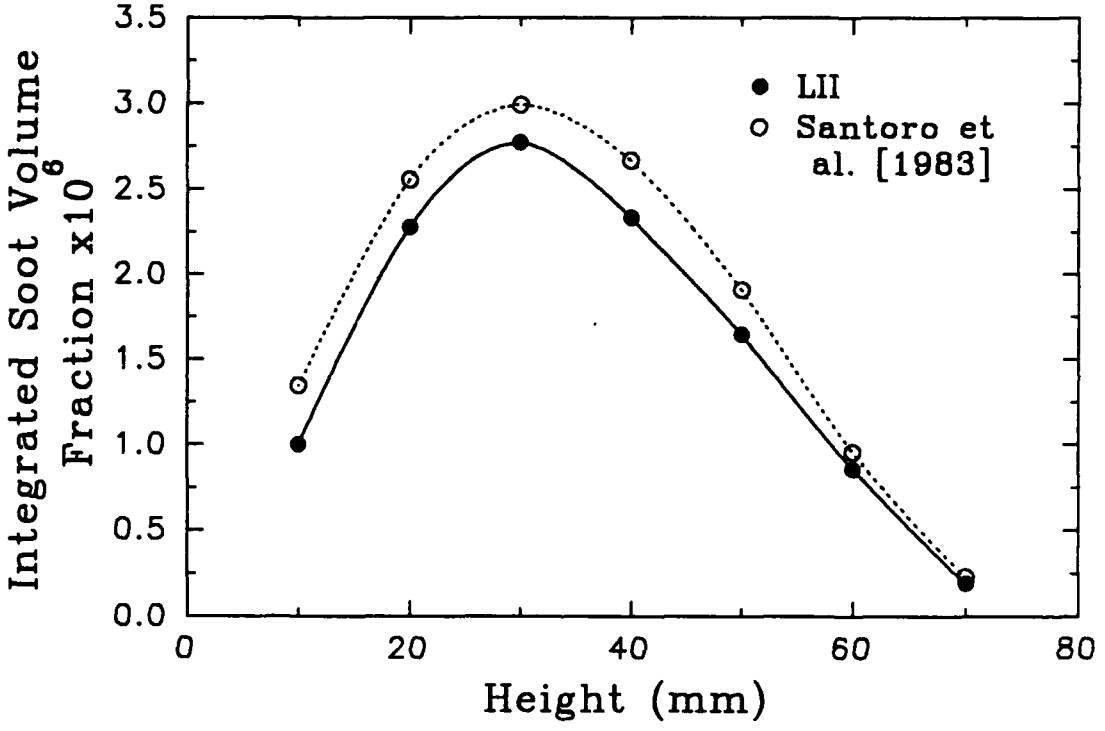
Integrated Soot Volume Fraction x10^6
3.5
3.0
2.5
2.0
1.5
1.0
0.5
0.0
0
20
40
60
80
Height (mm)
LII
Santoro et al. [1983]

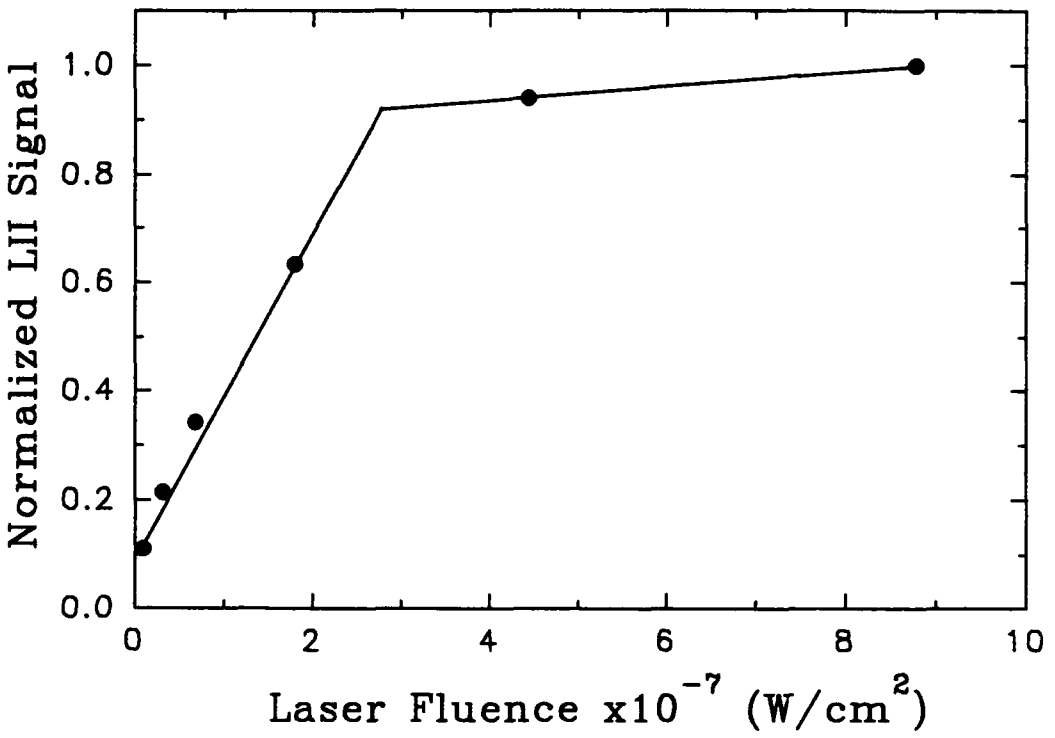
Normalized LII Signal
1.0
0.8
0.6
0.4
0.2
0.0
0
2
4
6
8
10
Laser Fluence x10^{-7} (W/cm^2)

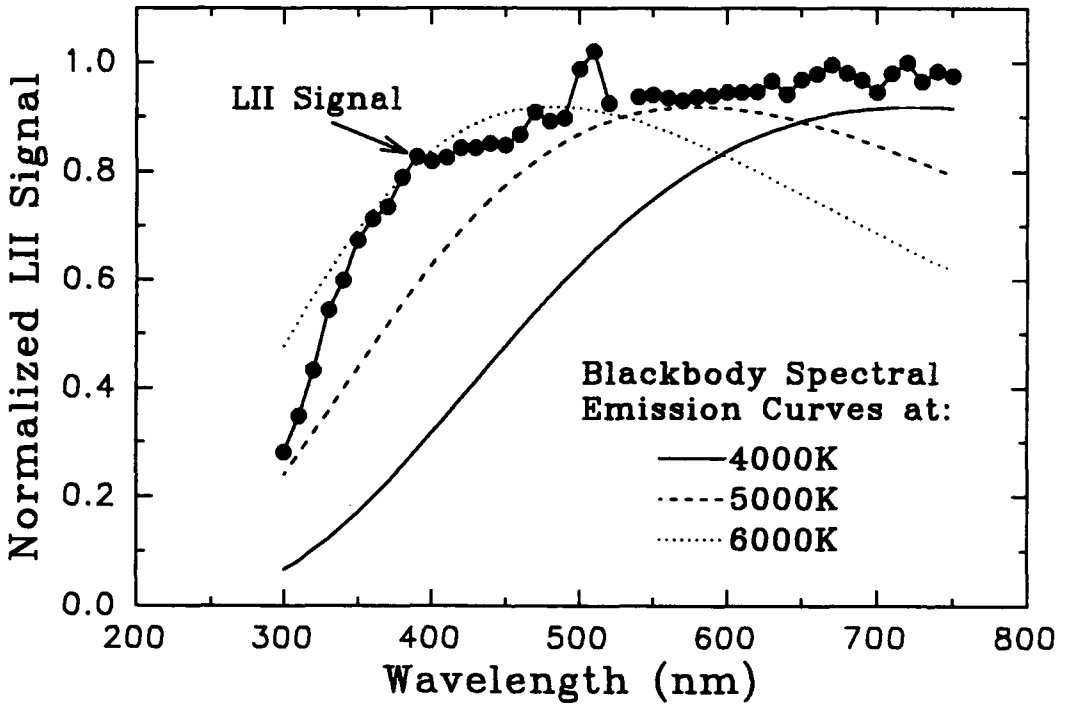
Normalized LII Signal
1.0
0.8
0.6
0.4
0.2
0.0
200
300
400
500
600
700
800
Wavelength (nm)
LII Signal
Blackbody Spectral
Emission Curves at:
4000K
5000K
6000K

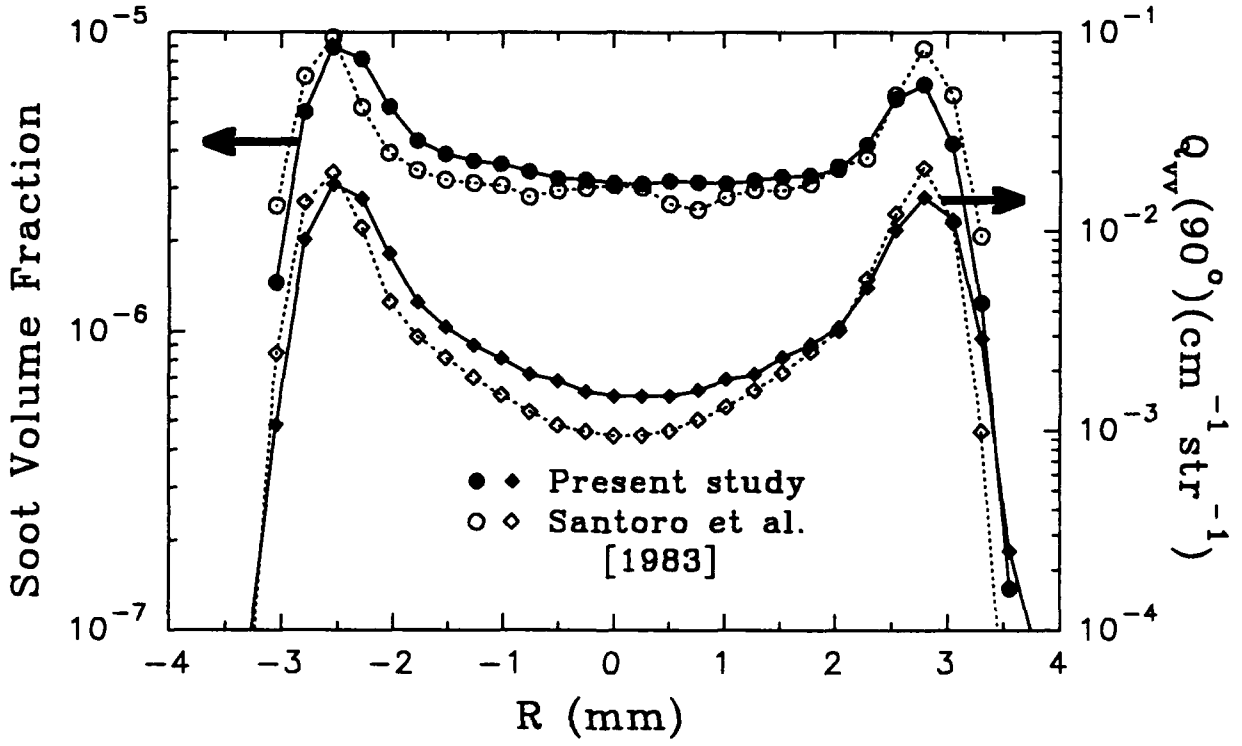
Soot Volume Fraction
10^{-5}
10^{-6}
10^{-7}
10^{-1}
10^{-2}
10^{-3}
10^{-4}
$q_{vv}(90^{\circ})(cm^{-1}str^{-1})$
−4 −3 −2 −1 0 1 2 3 4
R (mm)
Present study
Santoro et al. [1983]

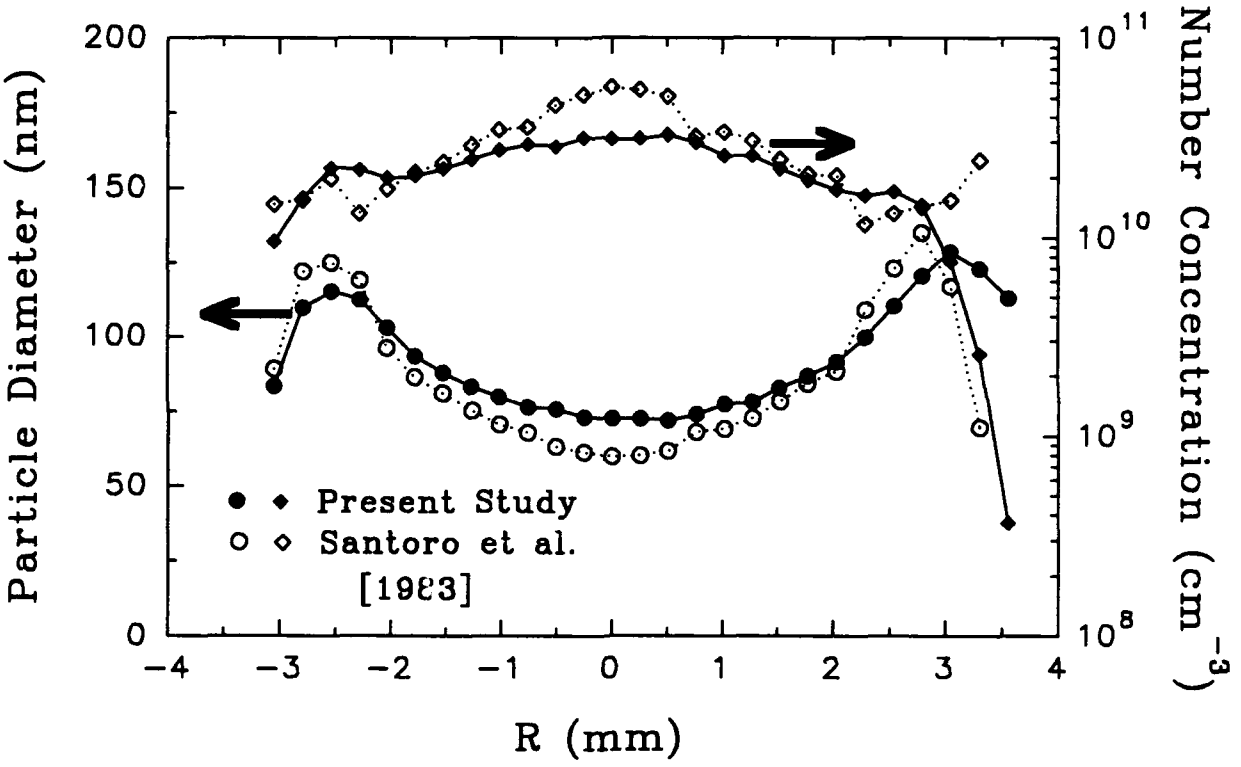
Particle Diameter (nm)
200
150
100
50
0
−4
−3
−2
−1
0
1
2
3
4
R (mm)
Number Concentration (cm^{-3})
10^{11}
10^{10}
10^{9}
10^{8}
Present Study
Santoro et al.
[1983]